European Journal of Pharmaceutical Sciences 175 (2022) 106209

Contents lists available at ScienceDirect

European Journal of Pharmaceutical Sciences

journal homepage: www.elsevier.com/locate/ejps

PLGA particle vaccination elicits resident memory CD8 T cells protecting from tumors and infection

Anna MacKerracher [a], Annette Sommershof [a], Marcus Groettrup [a,b,*]

[a] Division of Immunology, Department of Biology, University of Konstanz, 78457 Konstanz, Germany
[b] Biotechnology Institute Thurgau (BITg) at the University of Konstanz, 8280 Kreuzlingen, Switzerland

ARTICLE INFO

Keywords:
PLGA microspheres
Resident memory T cells
Vaccination
Lung
Tumor
Influenza A virus

ABSTRACT

The essential role of tissue-resident memory T cells (T_{RM} cells) in offering protection from recurring infections and malignant tumors is becoming increasingly clear. Due to their presence in many barrier tissues, T_{RM} cells are ideally located to rapidly respond to re-encountered pathogens. Moreover, a host of studies has shown that the quantity of T_{RM} cells correlates with increased survival rates in cancer patients. Therefore, vaccination strategies which induce a strong and sustained T_{RM} cell response are particularly promising. In this study we show that this response can be induced by employing a prime-boost vaccination strategy using biodegradable poly (D,L-lactide-*co*-glycolide) microspheres (PLGA MS). A subcutaneous prime immunization followed by an intranasal boost immunization led to a strong T_{RM} cell response in the lungs of mice 6 days after the boost vaccination. Although numbers subsequently declined, T_{RM} cells were still detectable 60 days after vaccination. Functionally, we observed that immunized mice were protected from lung metastasis formation and tumor growth in a B16Bl6 melanoma model. Furthermore, the T_{RM} cells induced by PLGA MS immunization provided protection in an infectious model using a recombinant influenza A virus (IAV). Taken together, these results show that the ability of PLGA MS to induce a strong T_{RM} cell response further supports their use as a potent vaccine.

1. Introduction

The ongoing COVID-19 pandemic has had an enormous impact on the world and highlights more than ever the need for effective vaccines. High efficacy requires the ability to induce long lasting and functionally efficient memory responses. Most currently employed vaccines mainly focus on inducing an antibody response, which can be suboptimal in several disease settings. The vaccines against influenza virus, for example, induce neutralizing antibodies that recognize the surface proteins hemagglutinin and neuraminidase (Wong and Webby, 2013). However, as these proteins are very prone to mutation due to antigenic drift, the influenza vaccine requires a yearly reformulation. In contrast to antibodies, the $CD8^+$ T cells response is mainly directed at internal virus proteins which are highly conserved (Gotch et al., 1987; McMichael et al., 1983). Therefore, more focus is being placed on the development of vaccines that induce a strong and long-lasting memory $CD8^+$ T cell response (Beura et al., 2018a). Research on memory $CD8^+$ T cells in the past has focused on the two main T cell memory subtypes found in the blood: central memory T cells (T_{CM} cells) and effector memory T cells (T_{EM} cells). T_{CM} cells circulate between lymph nodes (LNs) and the blood and are able to proliferate rapidly upon antigen recognition and thereby contribute to the new pool of effector T cells (T_{EFF} cells), whereas circulating T_{EM} cells circulate between the blood and non-lymphoid tissues and are ideally equipped to exert rapid effector functions (Sallusto et al., 2004). However, the recent discovery of a non-recirculating memory subtype, namely tissue-resident memory T cells (T_{RM} cells), has brought great advances to the field (Gebhardt et al., 2009; Masopust et al., 2010). T_{RM} cells have been found in barrier tissues, such as skin, lung, female reproductive tract, brain, liver, kidney, intestine, salivary glands and more recently also in primary and secondary lymphoid organs (Anderson et al., 2012; Beura et al., 2018b; Fernandez-Ruiz et al., 2016; Gebhardt et al., 2009; Jiang et al., 2012; Masopust et al., 2010; Schenkel et al., 2014; Wakim et al., 2008, 2010). They represent a very heterogeneous population which is strongly influenced by the microenvironment in the tissue of residence (Iijima and Iwasaki, 2015; Takamura, 2018). However, across tissues they share a common transcriptional phenotype and are often characterized by expression of CD69 and CD103 (Mueller and Mackay, 2016; Park and Kupper, 2015). Both proteins are involved in tissue retention: CD69 blocks expression of sphingosine-1-phosphate-receptor 1 (S1PR1) which is required to sense

* Corresponding author at: Division of Immunology, Universitaetsstr. 10, 78457 Konstanz, Germany.
E-mail address: marcus.groettrup@uni-konstanz.de (M. Groettrup).

https://doi.org/10.1016/j.ejps.2022.106209
Received 18 February 2022; Received in revised form 2 May 2022; Accepted 12 May 2022
Available online 15 May 2022

the S1P gradient in LNs and tissues that enables tissue egress (Mackay et al., 2015; Shiow et al., 2006). CD103 forms part of the integrin $\alpha_E\beta_7$ and thereby promotes tissue retention by binding to E-cadherin on epithelial cells (Pauls et al., 2001). Especially at barrier sites, T_{RM} cells provide front-line defense against re-encountered pathogens via direct effector mechanisms and recruitment of other immune cells from the blood (McMaster et al., 2015; Schenkel et al., 2013). Therefore, it is not surprising that the presence of T_{RM} cells has been found to correlate with a successful response to infectious diseases and increased protection from tumor growth (Marceaux et al., 2021; Muruganandah et al., 2018; Okła et al., 2021). Furthermore, due to their direct location in the tissue and their elevated expression of checkpoint molecules, such as programmed cell death protein 1 (PD-1), T_{RM} cells have been appointed ideally placed targets for immunotherapy (Corgnac et al., 2020; Edwards et al., 2018; Marceaux et al., 2021). In addition to their residency within the tissue and their ability to respond rapidly upon re-exposure to antigen, these cells are also in close contact with epithelial cells at risk of malignant transformation (Marceaux et al., 2021). Many vaccination strategies are thus being developed aimed at inducing a long-lasting T_{RM} cell response.

We and others have established a vaccination strategy based on encapsulation of antigens and adjuvants into poly-(D,L-lactic-*co*-glycolic) acid microspheres (PLGA MS). These polymers are hydrolyzed in aqueous solutions releasing the content, thus efficiently delivering the antigens to dendritic cells (DCs) in a targeted manner. PLGA MS can be taken up by various types of antigen-presenting cells (APCs) and the content can be presented via cross-presentation or MHC class II presentation to activate CD8+ and CD4+ T cells, respectively (Koerner et al., 2021; Schliehe et al., 2011). Since complete hydrolysis takes 30 days in the body, PLGA MS create a depot effect at the site of injection which leads to prolonged antigen presentation by DCs (Koerner et al., 2021). Moreover, encapsulation of antigens into these microparticles protects them from degradation (Johansen et al., 2000; Koerner et al., 2019; Waeckerle-Men and Groettrup, 2005). As antigenic peptides or proteins alone are not sufficient to induce a $CD8^+$ T cell response the addition of immunostimulatory adjuvants such as cytosine–phosphorothioate–guanine oligodeoxynucleotides (CpG ODN) or polyriboinosinic:polyribocitidylic acid (polyI:C) is required. These adjuvants need to be coencapsulated into the same PLGA MS to generate a vigorous immune response (Schlosser et al., 2008). Due to the excellent bioavailability, biodegradability and biocompatibility properties as well as the controlled release and low toxicity, PLGA has been licensed by the FDA and the EMA for pharmaceutical applications via the parenteral or mucosal route (Vasir, 2007). Furthermore, recent work from our group has just demonstrated that Riboxxim, a GMP-grade toll-like receptor (TLR) 3 /retinoic acid inducible gene I (RIG-I) ligand, is a potent immunostimulant that can be used in a clinical setting (Koerner et al., 2021). Moreover, a number of studies from our group have shown that immunization using PLGA MS was able to protect mice from tumor growth as well as virus infection (Herrmann et al., 2015; Koerner et al., 2021; Mueller et al., 2012, 2011).

In the present study we analyzed the memory $CD8^+$ T cells response following a subcutaneous (s.c.) prime – intranasal (i.n.) boost immunization with PLGA MS. We found that memory T cells, especially T_{RM} cells, were strongly induced in the lung interstitium and airways and while their numbers declined over time, they were still detectable 60 days after the boost immunization. Furthermore, we were able to show that these T_{RM} cells were functional and able to protect mice from tumor growth as well as infection with influenza A virus (IAV). Taken together, our data show that PLGA MS are efficient antigen delivery systems that are capable of inducing a strong, long-lasting local memory response.

2. Materials and methods

2.1. Preparation of PLGA MS

PLGA MS were prepared using 14 kDa PLGA 50:50 carrying hydroxyl- and carboxyl-end groups (Resomer ® RG502H, Evonik Röhm GmbH). The antigens Ovalbumin (Ova) (Sigma-Aldrich, 50 mg) or $M1_{58–66}$ peptide (peptides & elephants, sequence GILGFVFTL, 10 mg) and the TLR ligands CpG oligodeoxynucleotides with a phosphothioate backbone (CpG-ODN 1826, Microsynth, 5 mg) as well as polyI:C (Sigma-Aldrich, 0.5 mg) were dissolved in 0.5 ml 0.1 M $NaHCO_3$ (aqueous phase). For coencapsulation of antigens, such as Ova + CpG, both antigens were dissolved together in $NaHCO_3$. 1 g of PLGA was dissolved in 20 ml dichloromethane (organic phase). The aqueous and the organic phase were mixed by ultrasonication and immediately spray dried using the Mini Spray drier 191 (Büchi) at a flow rate of 2 ml/min at a room temperature of 25 °C. The obtained PLGA MS were washed out using 0.05% poloxamer 188 (Synperonic®F68, Serva Electrophoresis) and subsequently collected on a cellulose acetate membrane. The PLGA-MS were dried for 48 h in a vacuum drying cabinet at RT and stored at 4 °C until further use. Immediately before use they were dispersed in PBS by ultrasonication. The morphology and size distribution of PLGA MS were analyzed by scanning electron microscopy (SEM) (see Supplementary Fig. 1). Encapsulation and release kinetics as well as physicochemical characteristics for PLGA MS obtained in our laboratory by spray drying have previously been described (Herrmann et al., 2015; Koerner et al., 2021)

2.2. Animals

C57BL/6 mice and HLA-A*0201 transgenic mice (AAD mice) were originally obtained from Charles River, Germany. AAD mice express a recombinant MHC class I molecule consisting of the peptide binding region of the human HLA-A*0201 and the CD8 binding domain of the murine $H2\text{-}D^d$. Male and female mice were used at 8 - 12 weeks of age. All mice were kept in a specific pathogen-free environment on a 12/12 h light/dark cycle with *ad libitum* access to food and water. All experiments were approved by the review board of the Regierungspräsidium Freiburg (approval numbers: G-17/132, G-18/47, G-19/129, G-20/153, G-21/017, G-21/104).

2.3. Immunization

For s.c. prime immunization mice received a mixture of 5 mg PLGA MS containing CpG with or without the antigen together with 5 mg PLGA MS containing polyI:C dissolved in 200 µl PBS into the base of the tail. 14 days later mice received an i.n. boost vaccination. For i.n.l immunization mice received a mixture of 2.5 mg PLGA MS containing CpG with or without the antigen together with 2.5 mg PLGA MS containing polyI:C in a volume of 50 µl of PBS (25 µl/nostril). To ensure proper application of the i.n. vaccine and reduce stress levels mice were anesthetized with isoflurane (5% in oxygen; CP Pharma). The concentrations of the encapsulated antigens and TLR ligands per mouse were as follows: Subcutaneous immunizations: Ova (250 µg), $M1_{58–66}$ peptide (50 µg), CpG (25 µg) and polyI:C (2.5 µg). Intranasal immunizations: Ova (125 µg), $M1_{58–66}$ peptide (25 µg), CpG (12.5 µg) and polyI:C (1.25 µg).

2.4. Treatment with FTY720

Spingosine-1-phosphate-receptor 1 (S1PR1) inhibitor FTY720 (Sigma-Aldrich) was added to the drinking water of mice at indicated time points. Every 3 to 4 days the drinking water was exchanged with fresh water containing a new aliquot of the inhibitor. The concentration of the inhibitor was 7 µg/ml, leading to an approximate uptake of 1 mg/kg per day. To confirm the absence of circulating lymphocytes, blood was collected from the mice after they were sacrificed and analyzed by

flow cytometry staining for CD3.

2.5. Isolation of murine cells for flow cytometry

Immediately after sacrifice, blood was collected via heart puncture. Thereafter, a bronchoalveolar lavage was performed to obtain the bronchoalveolar lavage fluid (BALF). After collection of the spleen, mice were perfused using cold PBS to ensure removal of blood from the lungs. Spleens were gently mashed through a 40 μm strainer. Lungs were digested using the Lung Dissociation Kit, mouse (Miltenyi) and the gentleMACS Octo Dissociator with Heaters (Miltenyi) according to the manufacturer's protocol. Briefly, lungs were transferred to a gentleMACS C tube containing the enzyme mix (2.4 ml 1x Buffer S, 100 μl Enzyme D, 15 μl Enzyme A) and digested using the program "37C_m_LDK_1". Next, samples were filtered through a 70 μm MACS SmartStrainer and the C tubes were washed with 2.5 ml of Buffer S to minimize cell loss. After a 10-minute centrifugation step at 300 g, the supernatant was removed and the pellets were resuspended in FACS buffer for further use. All cell suspensions were lysed with erythrocyte lysis buffer (155 mM NH_4Cl, 10 mM $KHCO_3$, 0.1 mM EDTA) to ensure removal of erythrocytes before extracellular staining for flow cytometry.

2.6. Flow cytometry

For Tetramer analysis samples were stained with H-2−K^b $Ova_{257–264}$(SIINFEKL)-Tetramer or HLA-Ax0201 Influenza-$M1_{58–66}$ (GILGFVFTL)-Tetramer coupled to BV421 (MBL International Corporation, USA) for 30 min at room temperature (RT) protected from light. Subsequently, samples were incubated with the extracellular staining mix (Alexa Fluor 488-conjugated anti-CD8, BV711-conjugated CD44, APC-conjugated anti-CD62L, PE/Cy7-conjugated anti-CD69, PE-conjugated anti-CD103, BV605-conjugated CD127 and FVS620) in FACS buffer (1x PBS, 2% FCS, 2 mM EDTA) for another 30 min at 4 °C, before they were washed twice and subsequently analyzed on a BD LSRFortessa™ flow cytometer.

For determination of the T-lymphocyte reduction in the blood of FTY720-treated mice, blood samples were incubated with erythrocyte lysis buffer for 5 min to lyse erythrocytes. Following a washing step samples were stained with FVS780 and FITC-conjugated anti-CD3 in PBS for 30 min at 4 °C and subsequently washed with FACS buffer. Then samples were measured using a BD FACSVerse™ flow cytometer. Data was analyzed using FlowJo v10.7.1 software. The following antibodies were obtained from Biolegend: CD3 (clone 145–2C11), CD8 (clone 53–6.7), CD62L (clone MEL-14), CD69 (clone H1.2F3), CD127 (clone A7R34). The following antibodies were obtained from BD Biosciences: CD44 (clone IM7), CD103 (clone 2E7), FVS620 and FVS780.

2.7. Tumor cells

Ova^+Luc^+ B16BL6 cells were generated by lentiviral transduction of luciferase-expressing B16Bl6 cells with cytosolic Ova (amino acids 51–386). The original cell line B16BL6-luc+/GFP+ was kindly provided by Prof. Olaf van Tellingen (The Netherlands Cancer Institute, Amsterdam, The Netherlands). These cells were cultured in DMEM with 10% (v/v) FCS (both: Gibco, Thermo Fisher Scientific). To maintain luciferase expression, the growth medium was supplemented with 0.4 mg/ml G418 Sulfate (Geneticin™, Gibco, Thermo Fisher Scientific). 1×10^6 Ova^+Luc^+B16Bl6 tumor cells in PBS were injected intravenously 6, 18, 30 or 60 days after the i.n. boost immunization.

2.8. IVIS measurements

To monitor *in vivo* tumor growth in C57BL/6 mice measurements were performed using the IVIS200® System (Perkin Elmer). Measurements were done immediately following the injection of tumor cells and every 2–3 days thereafter for 24 days to follow the growth of lung metastases. Mice were anaesthetized by inhalation of 2.5% isoflurane before D-Luciferin*K (#bc219, Synchem) was injected i.p. at a concentration of 150 mg/kg. Bioluminescence was measured with a 20 cm field of view, small binning, and 120 s exposure time. Regions of interest (ROI) were preset around the signal on pseudo-color luminescent images using Living Image® v4.1 Software (Perkin Elmer). The emitted signal intensity (photon flux) was integrated over these ROIs and is expressed as relative light units (RLU, photons per second per cm^2) with the lower signal threshold set to 5% of the maximum signal value. Before each measurement mice were weighed to monitor their health status.

2.9. Influenza A virus amplification and infection

The recombinant Influenza A virus "insOva IAV" was kindly provided by Jonathan Yewdell (NIH, Bethesda, MD) (Dolan et al., 2010). It is a rPR8 strain expressing the SIINFEKL peptide in the stalk of NA [insOva]. insOva-IAV was amplified in Madin-Darby canine kidney (MDCK II) cells. Infection of mice with IAV was done at different time points after their boost immunization (6 or 30 days after the boost). Mice were anesthetized by inhalation of 5% isoflurane before they were i.n. inoculated with 1000 PFU of insOva-IAV. For determination of viral titers in the lungs mice were sacrificed 48 h after infection. Lungs were removed, weighed and 10 ml PBS added per 1 g of lung tissue. Subsequently, lungs were smashed through a 40 μm mesh and cell suspensions were frozen and thawed to ensure cell lysis and release of the virus. A plaque assay was performed to determine viral titers. For observation of bodyweight, mice were weighed daily starting from the day of infection. Mice were sacrificed once they had lost 20% of the initial bodyweight. When mice were euthanized the bodyweight at the endpoint was kept throughout the observation period.

2.10. Influenza a virus plaque assay

To determine the number of infectious particles in the lungs, a plaque assay was performed in 96-well plates as previously described (Herrmann et al., 2015; Matrosovich et al., 2006). Briefly, MDCK II cells were grown to confluence in 96-well plates before they were washed with PBS and infected with serial dilutions of the virus-containing samples (lung supernatants) in PBS for 60 min at 37 °C. After incubation, cells were overlaid with overlay-medium [1:1, MEM-medium:2.5% AVICEL® -Medium (FMC BioPolymer)] for 24 h. Next, virus-infected cells were washed and fixed with 4% Roti-Histofix (in PBS) for 30 min at 4 °C. Thereafter, cells were stained with a monoclonal antibody specific for the IAV nucleoprotein (Serotec) for 1 h at RT, followed by 1 h incubation with peroxidase-labeled anti-mouse antibody (DIANOVA) and 10 min incubation with True BlueTM peroxidase substrate (KPL, sera care). Stained plates were scanned on an Immunospot plate scanner (C.T.L. Europe). Viral titers are shown as the logarithm to the base 10 of the mean values.

2.11. Statistics

Statistical significance for comparison of multiple groups was determined by applying one-way or two-way analysis of variances (ANOVA) followed by Tukey's post-hoc tests. The Kaplan–Meier survival analysis was used to estimate statistical significance in overall survival distribution between the groups and Log-rank (Mantel–Cox) tests were applied to compare survival rates. The p values for experiment composites are given in the figure legends. All statistical analyses were performed using GraphPad Prism 9.0.0 software (GraphPad Software, Inc.).

3. Results

3.1. Prime-boost vaccination is highly efficient at inducing vaccine-specific T_{RM} cells in the lung

While many studies in the past years have investigated the generation of T_{RM} cells following different immunization or infection protocols none of these studies have used PLGA MS encapsulating antigens and adjuvants. Therefore, we set out to find the most efficient immunization protocol to generate a high number of T_{RM} cells in the lung using PLGA MS. While prior work has demonstrated that a mucosal route of vaccination is more efficient at inducing T_{RM} cells at mucosal sites than a systemic one, other studies have found that a combination of mucosal and systemic immunization yielded a stronger T_{RM} cell response than the mucosal one alone (Cuburu et al., 2012; Nizard et al., 2017; Sandoval et al., 2013; Uddback et al., 2016). We thus decided to compare four

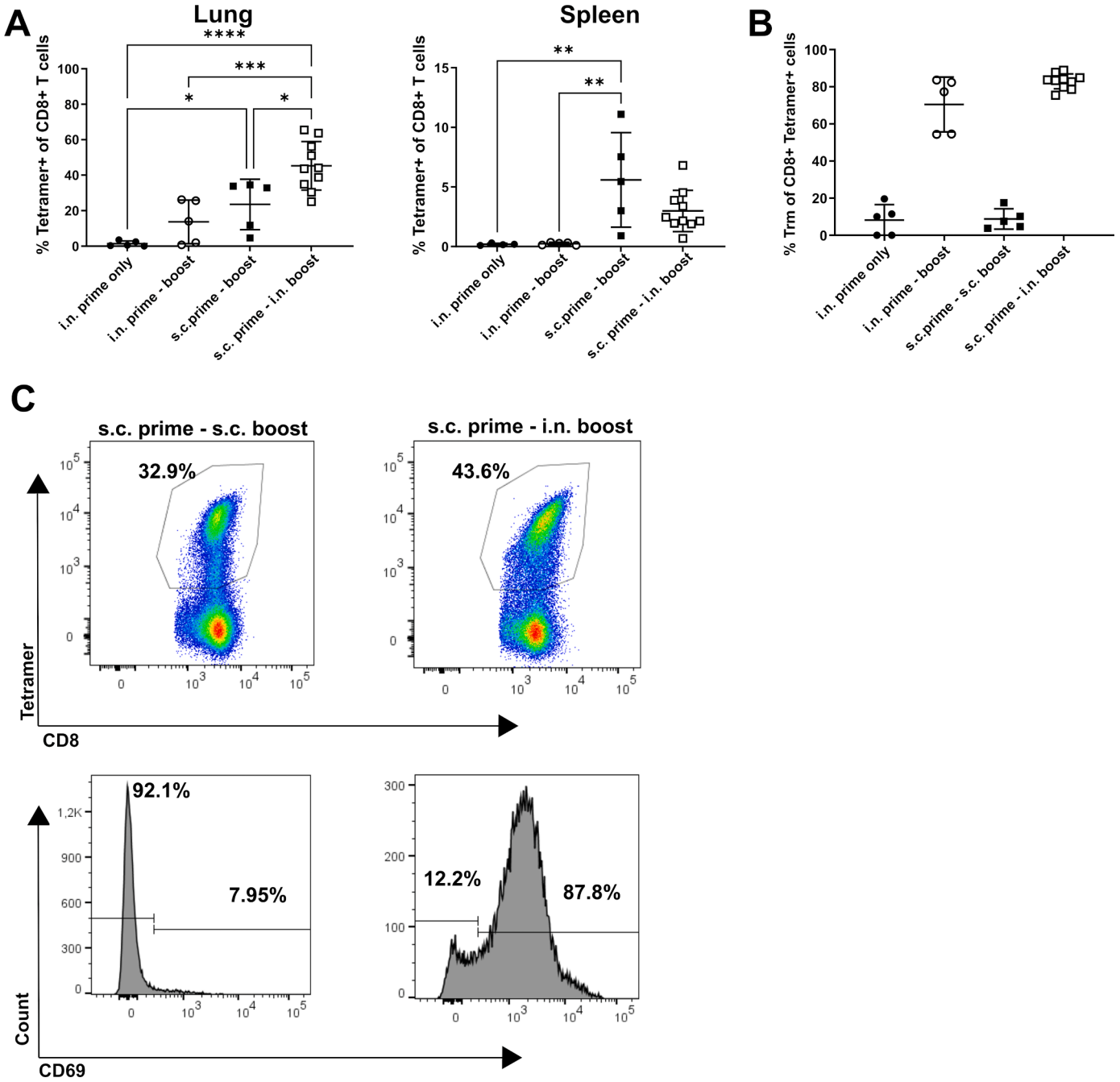

Fig. 1. s.c. prime – i.n. boost vaccination generates highest percentage of vaccine-specific $CD8^+$ T_{RM} cells.
C57BL/6 mice ($n = 5, 5, 5$ or 10) received a prime immunization on day 0. Depending on the protocol this was either an i.n. or an s.c. immunization using a mixture of PLGA MS containing Ova/CpG and PLGA MS containing polyI:C. For the prime – boost vaccination protocols mice received a boost vaccination on day 14. Lungs and spleen were removed on d6 after the last vaccination and analyzed for the presence of vaccine-specific $CD8^+$ T cells by flow cytometry. (A) The percentage of SIINFEKL-specific $CD8^+$ T cells ($Tetramer^+$) of all $CD8^+$ T cells is shown for lung and spleen for the different immunization protocols. (B) Percentage of $CD8^+$ $Tetramer^+$ T_{RM} cells ($CD62L^-CD69^+CD127^-$) of all $CD8^+$ SIINFEKL$^+$ T cells in the lung. Results are shown as mean ± SD. Statistics: one-way ANOVA with a Tukey's multiple comparisons test. *$p < 0.05$; **$p < 0.01$; ***$p < 0.001$; ****$p < 0.0001$. (C) Representative flow cytometry plots of the lung after immunization with the s.c. prime – s.c. boost (left) or the s.c. prime – i.n. boost (right) immunization strategy showing the percentage of Tetramer+ cells (top) and the expression of CD69 on those $Tetramer^+CD62L^-$ $CD69^+CD127^-$cells (bottom).

vaccination strategies: "i.n. prime only", "i.n. prime-boost", "s.c. prime-boost" and "s.c. prime-i.n. boost". This last strategy has previously been shown by our group to induce strong and sustained $CD8^+$ T cell responses, however no T_{RM} cells were analyzed in this study (Herrmann et al., 2015). To investigate T cell responses induced by the different vaccination regimens, lung and splenic lymphocytes were collected and analyzed for vaccine-specific $CD8^+$ responses 6 days after the last vaccination. Our results show that all three prime-boost immunization regimens were able to induce vaccine-specific $CD8^+$ T cells in the lung (Fig. 1A). However, the "s.c. prime – i.n. boost" immunization scheme resulted in significantly higher percentages of SIINFEKL-specific $CD8^+$ T cells in the lung compared to all other strategies. Similarly, the percentage of $CD69^+$ T_{RM} cells among $Tetramer^+$ (*i.e.* SIINFEKL-specific) $CD8^+$ T cells induced was also highest in the "s.c. prime – i.n. boost" vaccination group. Importantly, our results confirmed that an i.n. immunization was necessary to induce $CD69^+$ T_{RM} cells in the lung as the "s.c. prime – boost" strategy failed to induce cells with a T_{RM} cell phenotype despite the relatively high number of SIINFEKL-specific $CD8^+$ T cells (Fig. 1C). Taken together, our data show that a s.c. prime – i.n. boost immunization using PLGA MS is highly efficient at inducing T_{RM} cells in the lung. We therefore decided to continue all future experiments using this vaccination strategy.

3.2. PLGA MS-induced $CD8^+$ T cells in the lung are of the T_{RM} cell phenotype

Having established an ideal immunization scheme we next analyzed the generation of the different $CD8^+$ T cell subtypes in the lung and spleen 6 days after boost immunization (flow cytometry gating strategy: Supplementary Fig. 2). SIINFEKL-specific $CD8^+$ T cells were broken down into the previously described subtypes: effector T cells (T_{EFF}: $CD44^-$), central memory T cells (T_{CM}: $CD44^+$ $CD62L^+$ $CD69^-$), effector memory T cells (T_{EM}: $CD44^+$ $CD62L^-$ $CD69^-$) and resident memory T cells (T_{RM}: $CD44^+$ $CD62L^-$ $CD69^+$). Since T_{RM} cells, especially in mucosal tissues, often express CD103 we further looked at $CD103^+$ T_{RM} cells (Mueller and Mackay, 2016). Lung T_{RM} cells consist of two distinct populations: airway T_{RM}, which can be obtained by bronchoalveolar lavage (BAL) and interstitial T_{RM} cells, which are obtained by digestion of lung tissue (Takamura, 2017). In contrast to interstitial T_{RM} cells, airway T_{RM} cells are reported to be poorly cytolytic but able to produce antiviral cytokines rapidly after encountering their cognate antigen in a model of influenza infection (McMaster et al., 2015). Moreover, the number of airway T_{RM} cells has been shown to correlate with the efficacy of cellular immune protection in pulmonary infection (Wu et al., 2014). Therefore, we decided to analyze both populations of T_{RM} cells. Our data revealed that the pool of $CD8^+$ T cells in the lung airways predominantly consists of T_{RM} ($CD103^+$ and $CD103^-$) and T_{EM} cells (Fig. 2). As expected, a similar distribution was found in lung tissue, although the percentage of T_{RM} cells among $CD8^+Tetramer^+$ T cells was even higher compared to the airways. Interestingly, while we were not able to detect any effector T cells in the airways, there were some present in the lung tissue. As expected, we were not able to detect T_{CM} cells in either lung airways or tissue. In the spleen most of the vaccine-specific $CD8^+$ T cells represented a T_{EM} cell phenotype, although some T_{CM} cells as well as effector T cells were also detectable. Even though the $CD8^+$ T cells response was analyzed only 6 days after the boost vaccination, which represents the peak of the T cell response, most of the specific $CD8^+$ T cells in either of the tissues analyzed already displayed a memory phenotype. This is likely due to the fact that the systemic prime immunization 20 days before already led to the induction of an effector response. Moreover, it has been shown that T_{RM} cells (or their precursors) are present in the lung at very early time points after mucosal cancer vaccine administration (Nizard et al., 2017). In conclusion, these experiments establish that PLGA MS immunization leads to a strong induction of T_{RM} and T_{EM} cells in the lung airways and interstitium.

3.3. Availability of local antigen but not circulating T lymphocytes affects SIINFEKL-specific T_{RM} cell formation in the lung following PLGA MS immunization

After activation of lymphocytes in the LN, they are dependent on sphingosine-1-phosphate-(S1P)-dependent migration to exit the LN to traffic to the inflamed tissue (Matloubian et al., 2004). Treating mice with the sphingosine 1-phosphate receptor-1 (S1PR1) agonist FTY720 (Fingolimod) sequesters circulating T cells within secondary lymphoid tissues and thus prevents the migration of circulating lymphocytes into peripheral tissues (Brinkmann et al., 2002; Morris et al., 2005). Adding FTY720 to the drinking water of mice 2 days before the flow cytometric analysis enabled us to study the generation of local T_{RM} cells in the lung independently of circulating T cells. To confirm the impaired emigration of lymphocytes from secondary lymphoid organs in FTY720-treated mice, we first analyzed the frequency of $CD3^+$ T cells in the blood. As expected, we observed a significant reduction of circulating $CD3^+$ T lymphocytes in the blood of FTY720-treated mice (Supplementary

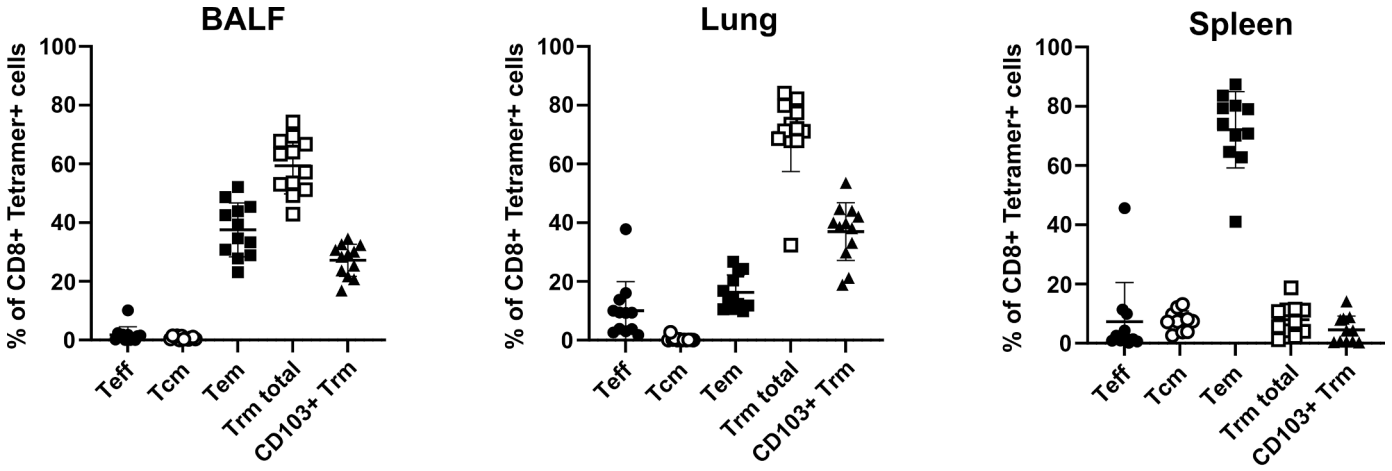

Fig. 2. PLGA MS vaccination induces $CD8^+$ T_{RM} cells in lung airway and interstitium.
C57BL/6 mice ($n = 12$) were immunized with the s.c. prime – i.n. boost immunization protocol using PLGA MS containing Ova/CpG which were co-administered together with PLGA-MS containing polyI:C. 6 days after the boost vaccination the bronchoalveolar lavage fluid (BALF), lung tissue and spleen were collected and analyzed by flow cytometry for the presence of vaccine-specific $CD8^+$ T cells. Graphs show the percentage of the different T cell subtypes of total $CD8^+$ $Tetramer^+$ cells. Results are shown as mean ± SD. Teff = effector T cells; Tcm = central memory T cells; Tem = effector memory T cells; Trm = tissue-resident memory T cells.

Fig. 3), confirming that emigration of these cells from lymphoid organs into the periphery was inhibited.

More importantly, there was no significant difference in the formation of $CD69^+CD103^+$ T_{RM} cell numbers in mice treated with the inhibitor (Ova/CpG/polyI:C + FTY720) compared to mice which did not receive the inhibitor (Ova/CpG/polyI:C), indicating that these cells were seeded in the lung already during the early phase of the vaccination response without further input from circulating $CD3^+$ T lymphocytes from the blood.

Another important aspect in the generation of T_{RM} cells is the requirement of antigen presence. In this context, it has been shown for several tissues, including the skin and the female reproductive tract (FRT) that local inflammation, but not local antigen, is required to induce T_{RM} cells (Casey et al., 2012; Mackay et al., 2012; Shin and Iwasaki, 2012). In the lung the situation seems to be different: without local antigen, T_{RM} cells that had been formed, did not persist after resolution of the inflammation (McMaster et al., 2018; Takamura et al., 2016).

Thus, we aimed to determine if local antigen presentation is a prerequisite for the establishment of a robust lung T_{RM} formation in the context of PLGA MS immunization. To this end, we used a prime-boost regimen in which mice were s.c. primed with PLGA MS containing Ova and the adjuvants (Ova/CpG/polyI:C) followed by the i.n. boost immunization without the antigen (CpG/polyI:C) on day 14 ("boost w/o antigen ± FTY720") and compared this group with mice receiving an i.n. boost immunization containing the antigen ("Ova/CpG/polyI:C ± FTY720"). 6 days after the boost immunization we analyzed the formation of vaccine-specific memory $CD8^+$ T cells in the lung airways, lung interstitium and the spleen (Fig. 3). In line with the previously mentioned work, our results confirm that while a local boost vaccination without antigen clearly induced a slight infiltration of $CD8^+$ T cells into the airways compared to mice immunized with empty PLGA MS, (Fig. 3A, left graph) it did not lead to the generation of vaccine-specific Tetramer+ $CD8^+$ T cells, especially that of T_{RM} cells in either of the sites analyzed. In contrast, a strong induction of total vaccine-specific $CD8^+$ T cells as well as T_{EM} and T_{RM} cells was observed in the lung airways (Fig. 3A) and tissue (Fig. 3B) of mice that received antigen-bearing PLGA microspheres both times. Interestingly, also in the spleen the boost w/o antigen strategy did not lead to a significant induction of $Tetramer^+$ $CD8^+$ T cells or T_{EM} cells (Fig. 3C). In summary, our results confirm that local antigen is required to induce efficient specific T_{RM} cells in the lung also in a vaccination approach using PLGA MS. However, when local antigen is present even mice that are no longer able to recruit lymphocytes from the circulation possess a significant number of T_{RM} cells in the lung.

3.4. Immunization with PLGA MS induces a sustained SIINFEKL-specific T_{RM} cell response in the lung

Since the main goal of a vaccine is to induce a long-lasting memory response we next longitudinally monitored the magnitude of the vaccine-induced memory $CD8^+$ T cell cells in the lung and spleen at different time points. Mice that had been immunized with PLGA MS according to the "s.c. prime – i.n. boost" vaccination approach were sacrificed 6, 18, 30 or 60 days after the boost vaccination and examined for the presence of $CD8^+$ memory T cells in the lung. While the numbers of all SIINFEKL-specific $CD8^+$ T cells and T_{RM} cells declined in the airways (Fig. 4A) and the interstitium (Fig. 4B), there were still specific memory $CD8^+$ T cells detectable even 60 days after the boost vaccination indicating that T cell memory did indeed persist. Also in the spleen we were able to find specific $CD8^+$ T cells, mainly T_{EM} cells, at this late time point however the overall response was lower than in the lung (Fig. 4C). Confirming our previous results, no differences were observable between mice treated with FTY720 compared to mice that did not receive the inhibitor, highlighting that the induced memory response in these mice could be maintained locally. It is interesting to note that the percentage of SIINFEKL-specific cells of all $CD8^+$ T cells strongly declined in the BALF and lung between day 30 and day 60 post boost in mice immunized with antigen-bearing PLGA MS treated with or without FTY720 (Fig. 4D). On the other hand, in the spleen the decline in SIINFEKL-specific $CD8^+$ T cells was gradual. This indicates that most specific $CD8^+$ T cells in the lung are lost approximately 1–2 months after boost immunization raising the potential need for a further boost immunization at a later time point. Moreover, we also studied the generation of T_{RM} cells following immunization with PLGA MS encapsulating the IAV peptide $M1_{58–66}$ and found similar results further highlighting that this strategy is capable of inducing T_{RM} cells specific to various antigens (Supplementary Fig. 4). Taken together, we show that the vaccine-specific $CD8^+$ T cell memory response in the lung following immunization with PLGA MS is maintained over a period of 2 months.

3.5. T_{RM} cells induced by immunization with PLGA MS protect mice from tumor growth

Having demonstrated that immunization with PLGA MS induces a robust population of T_{RM} cells in the lung, we next examined the capacity of these cells to protect mice from tumor growth. For this purpose, mice were immunized using the "s.c. prime – i.n. boost" vaccination protocol to ensure the induction of a robust memory $CD8^+$ T cell response in the lung. 6 days after the boost immunization, at the peak of the T cell response, we injected Ova- and luciferase-expressing B16Bl6 melanoma cells (Ova^+Luc^+B16Bl6) intravenously. This leads to the formation of metastases in the lung which can be tracked *in vivo* by measuring bioluminescence signals following i.p. injection of luciferin. In order to decipher the protection offered by the local immune response in the lung, we again included a group of mice that was treated with S1PR1-inhibitor FTY720. To allow enough time for local memory formation but prevent recruitment of circulating cells once tumor cells appeared in the lung, we commenced treatment with FTY720 two days before the injection of Ova^+Luc^+B16Bl6 cells. Our results clearly demonstrate that at this early time point mice immunized with antigen-bearing PLGA MS were strongly protected from tumor growth and metastasis formation even without the contribution of circulating $CD8^+$ T cells (Fig. 5A-C). Moreover, we observed that all groups of mice immunized with Ova exhibited an induction of T_{RM} cells in the lung as well as SIINFEKL-specific $CD8^+$ T cells in lung and spleen (Fig. 5D-F). Interestingly, mice that were immunized with adjuvant-containing PLGA MS ("CpG/polyI:C") also benefited from some level of protection compared to mice immunized with empty MS even though protection was not as efficient. Hence, in combination with local antigen provided by the tumor cells, inflammation alone was sufficient to induce an anti-tumor response. Next, we analyzed the protection offered by the local memory response in the lung at later time points. To this end, tumor cells were injected on day 18 (Fig. 6A), 30 (Fig. 6B) or 60 (Fig. 6C) post boost. While we observed that the protection clearly diminished over time, even 60 days after the boost mice were still to some extent protected against tumor growth indicating local long-term antitumor memory responses: basically no metastases were detected in mice that were able to make use of their local as well as their circulating vaccine-induced immune response even when the tumor challenge was performed 60 days post boost. Mice treated with FTY720 were protected from metastasis formation even when tumor cells were injected 30 days post boost, but were found to harbor some metastases in their lungs at the last time point analyzed (Fig. 6*A*+*B* + C, middle graphs). This same tendency was also seen for the bioluminescence measurements (Fig. 6*A*+*B* + C, left graphs). While lower bioluminescence signals were obtained in both groups immunized with Ova-bearing PLGA MS compared to unprotected mice, this effect grew smaller over time. However, there still seems to be some kind of lung resident protection since the mice exhibited less tumor formation than mice that had not been immunized with antigen-bearing PLGA MS. Interestingly, all groups of mice that were immunized with at least the adjuvants

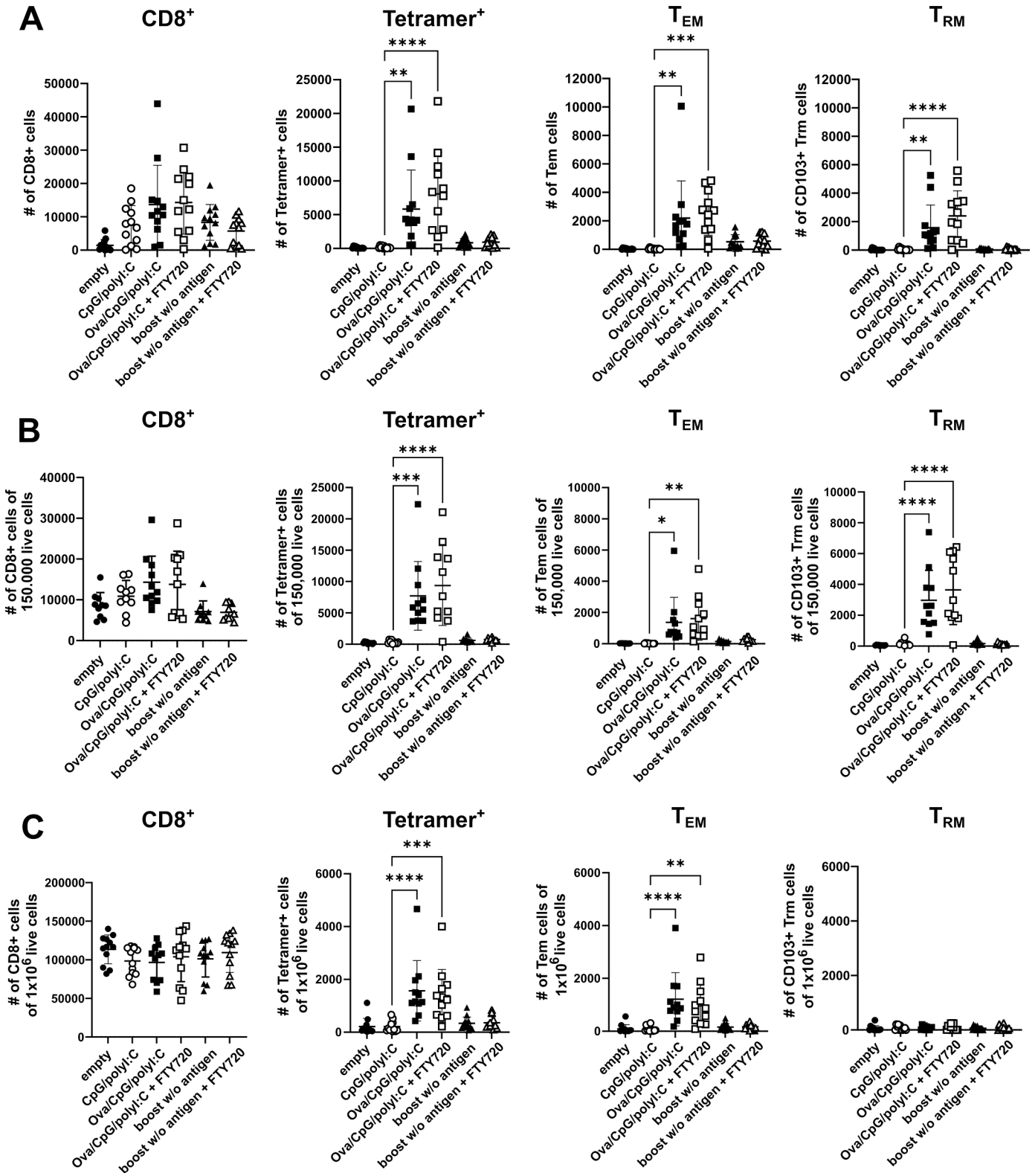

Fig. 3. Local antigen is required for induction of $Ova_{257–264}$-specific $CD8^+$ T_{RM} cells in the lung.
C57BL/6 mice ($n = 12$) were immunized with the s.c. prime – i.n. boost immunization protocol using PLGA MS containing Ova/CpG which were co-administered together with PLGA MS containing polyI:C. The "boost w/o antigen" groups received antigen-bearing PLGA MS (Ova/CpG/polyI:C) for their s.c. prime immunization, but were i.n. boosted with adjuvant-only PLGA MS (CpG/polyI:C). The S1PR1-inhibitor FTY720 was added to the drinking water (7 μg/ml) of the indicated groups two days before analysis. Control groups were immunized with either empty PLGA MS or adjuvant-only PLGA MS (CpG/polyI:C) for prime and boost vaccination. Absolute cell count of $CD8^+$ cells, $CD8^+$ $Tetramer^+$ cells, T_{EM} cells or $CD103^+$ T_{RM} cells in the BALF (A), lung (B) or spleen (C). (B) Cell numbers in the lung were normalized to 150,000 live cells. (C) Cell numbers in the spleen were normalized to 1×10^6 live cells. Results are shown as mean ± SD. Statistics: one-way ANOVA with a Tukey's multiple comparisons test. Only the significant differences between Ova/CpG/polyI:C or Ova/CpG/polyI:C + FTY720 to CpG/polyI:C are shown. $^*p < 0.05$; $^{**}p < 0.01$; $^{***}p < 0.001$; $^{****}p < 0.0001$.

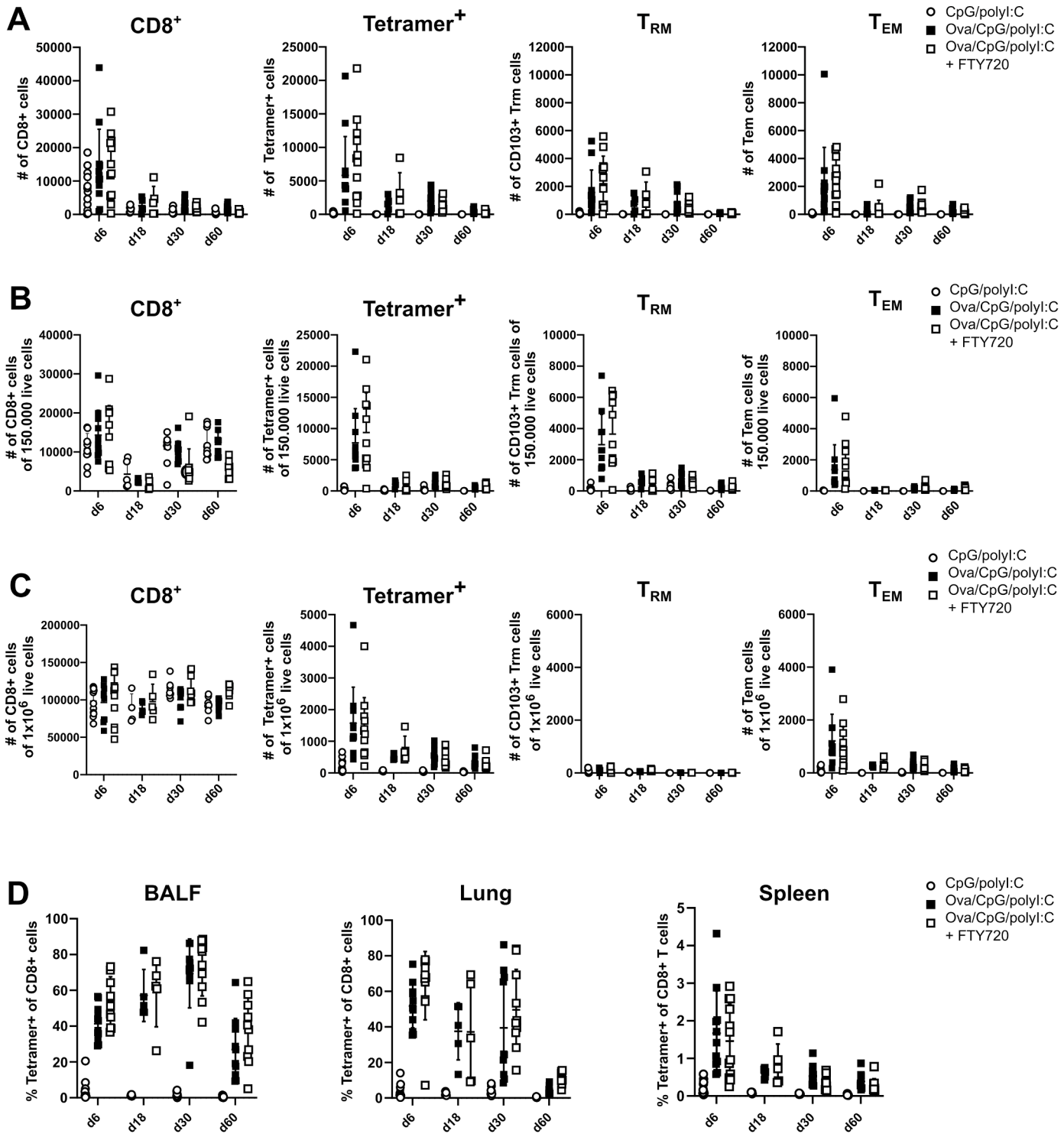

Fig. 4. The vaccine-specific memory $CD8^+$ T cell response in the lung persists for up to 60 days.
C57BL/6 mice ($n = 12$) were immunized with the s.c. prime – i.n. boost immunization protocol using PLGA MS containing Ova/CpG which were co-administered together with PLGA MS containing polyI:C. The S1PR1-inhibitor FTY720 was added to the drinking water (7 μg/ml) of the "Ova/CpG/polyI:C + FTY720" group two days before analysis. The control group was immunized with adjuvant-only PLGA MS (CpG/polyI:C). Mice were sacrificed 6, 18, 30 or 60 days after the boost immunization. (A-C) Cell count of $CD8^+$, $CD8^+$ $Tetramer^+$, T_{EM} cells or $CD103^+$ T_{RM} cells in the BALF (A), lung (B) or spleen (C). (B) Cell numbers in the lung were normalized to 150,000 live cells. (C) Cell numbers in the spleen were normalized to 1×10^6 live cells. (D)% $Tetramer^+$ cells of all $CD8^+$ T cells in BALF, lung and spleen. Results are shown as mean ± SD.

displayed an increase in SIINFEKL-specific $CD8^+$ T cells in lung and spleen and T_{RM} cells in the lung compared to the "empty" control mice which suggests that inflammation alone strongly induces the formation of specific $CD8^+$ T cells as long as the antigen is provided by the tumor (Fig. 6*A*+*B* + C, right graphs). Consequently, these results illustrate that the local memory response generated by prime-boost immunization with PLGA MS is capable of inducing protective anti-tumor responses in mice.

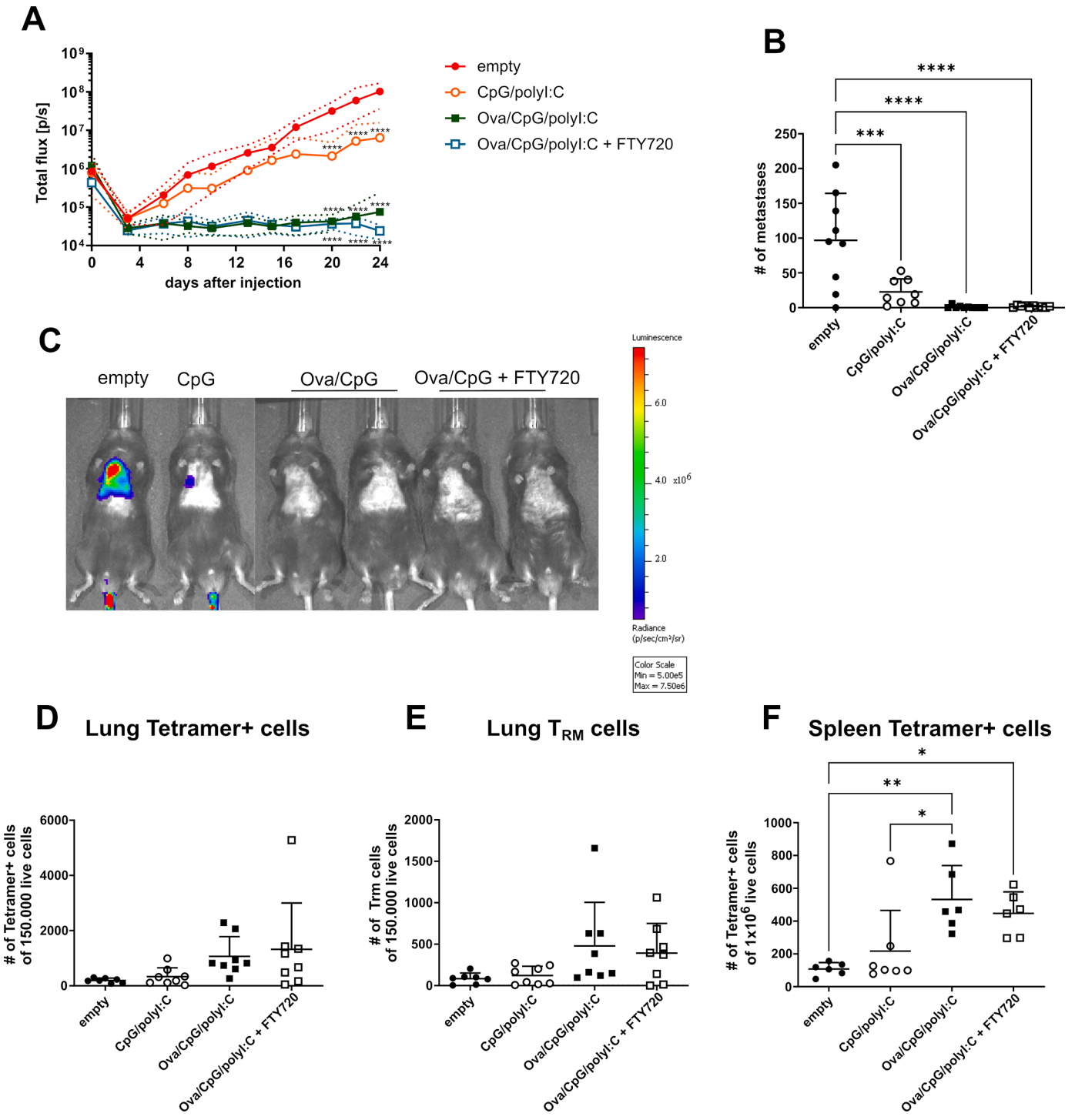

Fig. 5. T_{RM} cells induced by PLGA MS protect mice from tumor growth.
C57BL/6 mice ($n = 6–8$) were immunized with the s.c. prime – i.n. boost immunization protocol using PLGA MS containing Ova/CpG which were co-administered together with PLGA MS containing polyI:C. Control groups were immunized with either empty PLGA MS or adjuvant-only PLGA MS (CpG/polyI:C). 6 days after the boost immunization Ova^+Luc^+B16Bl6 melanoma cells were injected *i.v.* into the tail vain. FTY720 was added to the drinking water (7 μg/ml) of mice in the "Ova/CpG/polyI:C + FTY720" group 2 days before injection of the tumor cells. (A) Total flux of tumor bioluminescence of Ova^+Luc^+B16Bl6 cells shown as photons/second. Data are presented as mean ± S.D. with dotted lines in corresponding colors demonstrating individual data variances. Statistics: two-way ANOVA with a Tukey's multiple comparisons test. Statistical significances compared to "empty" group. (B) Number of metastases counted in the lung 24 days after injection of tumor cells. Statistics: one-way ANOVA with a Tukey's multiple comparisons test (C) Representative IVIS® images demonstrating tumor growth 24 days after PLGA MS boost immunization. Scaling of the bioluminescent pseudo-color code is shown and presented as photons/seconds/cm2/steradian (p/sec/cm/sr). (D-F) Number of $CD8^+$ $Tetramer^+$ cells in lung (D) and spleen (F) and $CD8^+$ $Tetramer^+CD62L^-$ $CD69^+CD127^-$ T_{RM} cells in the lung (E). Statistics: one-way ANOVA with a Tukey's multiple comparisons test. Results are shown as mean ± SD. $^*p < 0.05$; $^{**}p < 0.01$; $^{***}p < 0.001$; $^{****}p < 0.0001$.

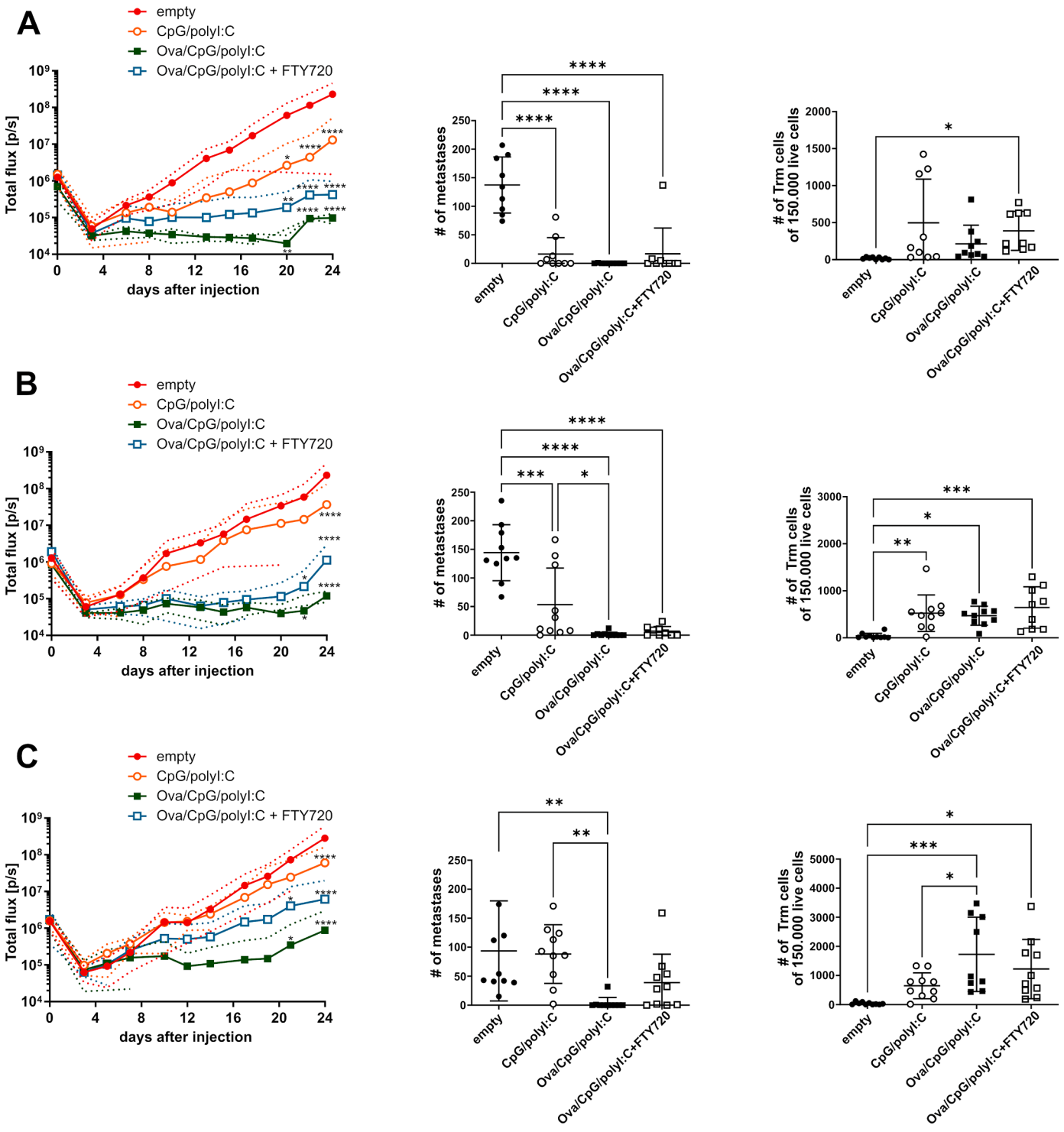

Fig. 6. Immunization with PLGA-MS induces long-lasting protection from tumor growth.
C57BL/6 mice ($n = 9$–10) were immunized with the s.c. prime – i.n. boost immunization protocol using PLGA MS containing Ova/CpG which were co-administered together with PLGA MS containing polyI:C. Control groups were immunized with either empty PLGA MS or adjuvant-only PLGA MS (CpG/polyI:C). 18 (A), 30 (B) or 60 (C) days after the boost immunization Ova^{+}Luc^{+}B16Bl6 melanoma cells were injected *i.v.* into the tail vain. FTY720 was added to the drinking water of mice in the "Ova/CpG/polyI:C + FTY720" group 2 days before injection of the tumor cells (7 μg/ml). (left graphs) Total flux of tumor bioluminescence of Ova^{+}Luc^{+}B16Bl6 cells shown as photons/seconds. Data are presented as mean ± S.D. with dotted lines in corresponding colors demonstrating individual data variances. Statistics: two-way ANOVA with a Tukey's multiple comparisons test. Statistical significances compared to "empty" group. (middle graphs) Number of metastases counted in the lung 24 days after injection of tumor cells. Statistics: one-way ANOVA with a Tukey's multiple comparisons test. (right graphs) Number of CD8^{+}Tetramer^{+} CD62L^{-} CD69^{+}CD127^{-} T_{RM} cells in the lung. Results are shown as mean ± SD. Statistics: one-way ANOVA with a Tukey's multiple comparisons test. *$p < 0.05$; **$p < 0.01$; ***$p < 0.001$; ****$p < 0.0001$.

3.6. T_{RM} cells induced by immunization with PLGA MS protect mice from influenza infection

It has long been known that T_{RM} cells are able to offer optimal protection not only from tumor growth but also from infection (Muruganandah et al., 2018). Therefore, we analyzed the protective response in a model of influenza infection. The induction of a long-lasting T_{RM} cell response directed at internal, conserved viral proteins might offer heterosubtypic protection from different influenza virus strains and is thus a desirable feature of a newly developed vaccine (Gotch et al., 1987; McMichael et al., 1983). Thus, following our established prime-boost immunization scheme we infected mice with the recombinant IAV strain expressing SIINFEKL in the stalk of the neuraminidase protein (insOva IAV). When mice were infected 6 days post boost, we observed a significant reduction in body weight loss compared to control mice receiving either "empty" PLGA MS or PLGA MS containing only

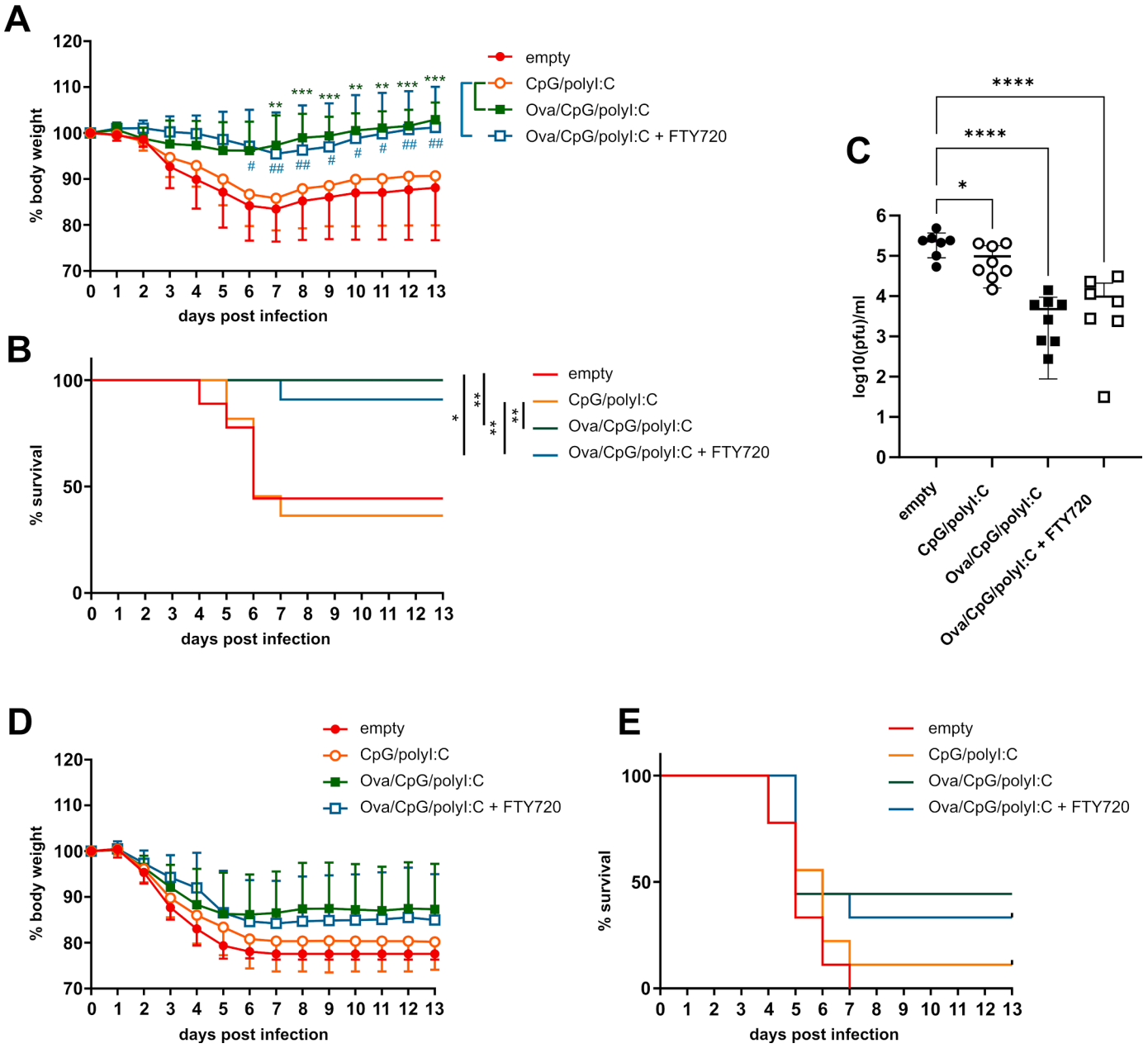

Fig. 7. T_{RM} cells induced by PLGA MS protect mice from influenza infection.
C57BL/6 mice ($n = 7$–10) were immunized with the s.c. prime – i.n. boost immunization protocol using PLGA MS containing Ova/CpG which were co-administered together with PLGA MS containing polyI:C. Control groups were immunized with either empty PLGA MS or adjuvant-only PLGA MS (CpG/polyI:C). 6 (A-C) or 30 (*D + E*) days after the boost immunization mice were i.n. infected with 1000 PFU of insOva-IAV. FTY720 was added to the drinking water of mice in the "Ova/CpG/polyI:C + FTY720" group 2 days before infection (7 μg/ml). (*A + D*) Body weight was measured every day for a period of 13 days and obtained values were calculated in relation to the weight on the day of infection. Mice were sacrificed once they had lost 20% of the initial bodyweight. When mice were euthanized the last recorded bodyweight at the endpoint was used throughout the observation period. Statistical significances show results for the "Ova/CpG/polyI:C group (green) or the "Ova/CpG/polyI:C + FTY720" group (blue) compared to "CpG/polyI:C" group. Statistics: two-way ANOVA with a Tukey's multiple comparisons test. (*B + E*) Kaplan-Meier survival curves of mice after infection with influenza. Statistics: Log-rank (Mantel–Cox) tests. (C) Virus titer in the lung of mice that were sacrificed 48 h after infection. Statistics: one-way ANOVA with a Tukey's multiple comparisons test. Results are shown as mean ± SD. *$p < 0.05$; **$p < 0.01$; ***$p < 0.001$; ****$p < 0.0001$. (For interpretation of the references to colour in this figure legend, the reader is referred to the web version of this article.)

"CpG/polyI:C" (Fig. 7A). In line with this observation, mice immunized with antigen-bearing PLGA MS were protected from influenza-induced death, while in the control groups more than 50% of the mice had to be sacrificed due to excess weight loss (Fig. 7B). Mice immunized with Ova-containing PLGA MS also exhibited a significantly reduced viral titer in the lung 48 h after infection confirming that prime-boost immunization with antigen-bearing PLGA MS resulted in a more rapid clearance of the virus than in control mice (Fig. 7C). Importantly, mice that were treated with FTY720 to prevent the recruitment of circulating lymphocytes showed no significant difference compared to mice that were able to make use of the recruitment of circulating lymphocytes, indicating that the locally established immune response in the lung was sufficient to avert virus infection. To investigate whether the PLGA MS induced virus-specific immune response could also protect against influenza virus infection in the long term, we infected mice 30 days after the i.n. boost immunization. Our results show that mice immunized with antigen-bearing PLGA MS treated with or without the inhibitor FTY720 exhibited superior protection against respiratory influenza challenge compared to control mice, although this protection was not significant and not sufficient to prevent virus-induced weight loss and death in the majority of mice (Fig. 7*D*+*E*). Nevertheless, mice treated with FTY720 were protected from influenza infection in a similar manner to Ova-immunized mice not treated with the inhibitor suggesting that protection is mediated by lung resident memory $CD8^+$ T cells and does not rely on replenishment from the periphery. In summary, these results show that PLGA MS are capable of inducing local memory responses sufficient to enhance virus clearance and protect mice from lethal influenza challenge at an early time point after immunization.

4. Discussion

There is now a plethora of data highlighting the great immunological potential of T_{RM} cells. While T_{RM} cells were originally found to offer protection from infections, more recent data also showed their essential role in antitumor immunity. In line with this, several studies have found a correlation of T_{RM} cells numbers and the overall survival rate in various tumors (Djenidi et al., 2015; Koh et al., 2017; Komdeur et al., 2017; Marceaux et al., 2021; Zens et al., 2016). Therefore, the development of a vaccine that is able to elicit a strong T_{RM} response is very desirable. PLGA MS are an ideal candidate for such a vaccination strategy as they are approved for application via the mucosal route and the requirement for a mucosal application to efficiently generate T_{RM} cells has been demonstrated in multiple settings (Cuburu et al., 2012; Nizard et al., 2017; Sandoval et al., 2013). Here we confirm that a mucosal route of immunization is required for the generation of vaccine-specific $CD8^+$ T cells with a T_{RM} cell phenotype. Interestingly, we find that the combination of a systemic prime immunization followed by a local boost induces the highest percentages of total vaccine-specific $CD8^+$ T cells as well as T_{RM} cells in the lung. Additionally, this strategy also induces a robust specific $CD8^+$ T cell response in the spleen. As it has been suggested that a circulating antigen-specific T cell population may be important to back up the local response if needed, the simultaneous induction of both systemic and local antigen-specific cells with PLGA MS using our immunization strategy is very promising (Uddback et al., 2016).

The release kinetics of encapsulated antigens from PLGA MS have shown a characteristic burst release within the first 24 h after administration, followed by continuous degradation of the polymer and a concomitant release of the protein or peptide antigen over a period of about 30 days. This depot effect prolongs T cell stimulation (Koerner et al., 2021). Making use of the controlled and joint release of antigens together with adjuvants, PLGA has been broadly used for cancer immunotherapy in preclinical settings (Hamdy et al., 2011). Monoclonal antibodies targeting immune checkpoint molecules, such as PD-1 or Cytotoxic T-Lymphocyte-Associated Protein 4 (CTLA-4), have been approved by the FDA and EMA for treatment in different cancers and have greatly improved the therapeutic success of cancer immunotherapy. However, efficient immune checkpoint blockade requires pre-existing cancer-specific cytotoxic $CD8^+$ T lymphocytes to be present at the tumor site (Ribas and Wolchok, 2018). Recent work from our group has demonstrated that PLGA MS were able to induce antitumor responses which were synergistically enhanced by immune checkpoint blockade (Koerner et al., 2021). Since T_{RM} cells have been shown to express high levels of immune checkpoint molecules such as PD-1, they have been proposed as ideal targets for immune checkpoint blockade therapy (Corgnac et al., 2020; Edwards et al., 2018; Marceaux et al., 2021). This further highlights the benefits of inducing T_{RM} cells with a vaccination strategy.

In this study we show that a s.c. prime followed by an i.n. boost immunization led to a strong memory response in the lung airways and interstitium with the majority of cells possessing a T_{RM} cell phenotype. In line with prior work, we observed that even though a memory response was still detectable at later time points, numbers of T_{RM} cells had declined substantially. This is a common theme for lung T_{RM} cells: airway T_{RM}, which are especially short-lived, have been found to possess a half-life of only 14 days which is likely due to the inhospitable environment in the airways (Hayward et al., 2020). But also interstitial T_{RM} cells are not as long-lasting as T_{RM} cells in other tissues, such as the skin where they can persist up to a lifetime in mice (Slütter et al., 2017; Zaid et al., 2014). While T_{RM} cells in the skin occupy niches that offer ideal conditions for these cells, $CD8^+$ T_{RM} cells in the lung are enriched in specific niches created at the site of tissue regeneration after injury which have been termed repair-associated memory depots (RAMDs) (Takamura, 2018; Takamura et al., 2016). These niches slowly disappear with the recovery of the tissue. Since the tissue injury induced by immunization with PLGA MS is clearly not as prominent as that induced in an infectious or tumorous setting this might offer an explanation for the sooner decline in numbers in our vaccination setting. However, prior studies have demonstrated that repeated influenza infections were able to induce T_{RM} cells that persisted in larger numbers and were resistant to apoptosis (Van Braeckel-Budimir et al., 2018). Moreover, we have previously shown that a boost immunization 8 weeks after the prime could strongly enhance the $CD8^+$ T cell response (Herrmann et al., 2015). Collectively, these results suggest that an additional boost vaccination at later time points might be necessary and might lead to a sustained T_{RM} cell response. However, it is important to keep in mind that the strong decline in T_{RM} cell numbers in the lung in comparison to other tissues seems to fulfill a protective function. The main function of the lung tissue is gas exchange which might be compromised by the accumulation of vast numbers of immune cells (Takamura, 2017). Therefore, the benefit of additional boost immunizations to induce a more long-lasting T_{RM} cell populations in the lung has to be studied carefully.

Having validated that immunization with PLGA MS was able to induce a strong local immune response in the lung, we went on to demonstrate that this local memory response was able to offer protection in a tumor model as well as an infectious model. While we were able to demonstrate that the local memory response was clearly capable of providing sufficient protection in both disease models at an early time point, our data also indicates that the protection provided only by the local immune response was not sufficient at later time points. The protective response of mice which were only able to make use of their local memory populations started to decline sooner than in those mice that were able to additionally make use of the circulating T cell population. The observation that both the local as well as the circulating T cell populations are required for optimal immune responses has also been made by other groups (Nizard et al., 2017). Considering that one of the main mechanisms by which T_{RM} cells are known to offer protection from reinfection is via recruitment of circulating immune cells, this is not an unexpected finding (Schenkel et al., 2013). Nonetheless, even at later time points the resident memory response still offered some protection compared to unprotected control mice.

Even despite the fact that T_{RM} cell numbers and protection declined,

PLGA MS still offer some great potential. One of the main challenges regarding vaccination against influenza viruses is the need for a yearly reformulation of the vaccine due to the high mutation rate of the epitopes recognized by the antibodies which are elicited by the currently employed influenza vaccines. This requires the prediction of the most likely circulating virus strains a few months before the start of the next influenza season. In the case of a mismatch between the vaccine and the circulating strain vaccine efficacy is considerably lower (Krammer et al., 2018). Since $CD8^+$ T cells have been shown to offer heterosubtypic protection from influenza virus and PLGA MS are able to induce a strong influenza-specific $CD8^+$ T cell response, this suggests that the same vaccine formulation could be used for a yearly boost immediately before the season circumventing the problem of a potential vaccine – strain mismatch. Moreover, we have previously shown that several epitopes can be encapsulated into the same PLGA MS further reducing the risk of a potential loss of vaccination efficacy due to antigenic drift of the influenza virus (Herrmann et al., 2015).

Taken together, we provide evidence that a vaccination strategy using PLGA MS has the capacity to induce a strong T_{RM} response in the lung. PLGA-based particles have previously been shown to induce T_{RM} cells in the lung that are capable of protecting mice from influenza infection (Kingstad-Bakke et al., 2021). Here we were able to confirm these results and further show that the induced T_{RM} cells were also able to protect mice from tumor growth in a tumor model. Therefore, our results further support the use of PLGA MS-based vaccination approaches for immunotherapy and influenza vaccination.

Funding

This project has received funding from the German Ministry of Education and Research (BMBF) grant Nr. 01KC2010A.

CRediT authorship contribution statement

Anna MacKerracher: Conceptualization, Investigation, Visualization, Writing – original draft. **Annette Sommershof:** Conceptualization, Writing – review & editing, Supervision, Funding acquisition. **Marcus Groettrup:** Conceptualization, Writing – review & editing, Supervision, Funding acquisition.

Declaration of Competing Interest

None.

Acknowledgement

We would like to thank Dennis Horvath for preparing the graphical abstract. We also want to thank the flow cytometry facility FlowKon, the Electron Microscopy Center (EMC), in particular Michael Laumann, and the Animal Research Center at the University of Konstanz for help and guidance. We thank Olaf van Tellingen for the contribution of the Luc+ B16Bl6 cell line and Jonathan Yewdell for providing us with the recombinant IAV.

Supplementary materials

Supplementary material associated with this article can be found, in the online version, at doi:10.1016/j.ejps.2022.106209.

References

Anderson, K.G., Sung, H., Skon, C.N., Lefrancois, L., Deisinger, A., Vezys, V., Masopust, D., 2012. Cutting edge: intravascular staining redefines lung CD8 T cell responses. J. Immunol. 189, 2702–2706.

Beura, L.K., Jameson, S.C., Masopust, D., 2018a. Is a Human CD8 T-cell vaccine possible, and if So, what would it take? CD8 T-cell vaccines: to B or not to B? Cold Spring Harb. Perspect. Biol. 10.

Beura, L.K., Wijeyesinghe, S., Thompson, E.A., Macchietto, M.G., Rosato, P.C., Pierson, M.J., Schenkel, J.M., Mitchell, J.S., Vezys, V., Fife, B.T., Shen, S., Masopust, D., 2018b. T Cells in Nonlymphoid tissues give rise to Lymph-Node-Resident memory T cells. Immunity 48, 327–338 e325.

Brinkmann, V., Davis, M.D., Heise, C.E., Albert, R., Cottens, S., Hof, R., Bruns, C., Prieschl, E., Baumruker, T., Hiestand, P., Foster, C.A., Zollinger, M., Lynch, K.R., 2002. The immune modulator FTY720 targets sphingosine 1-phosphate receptors. J. Biol. Chem. 277, 21453–21457.

Casey, K.A., Fraser, K.A., Schenkel, J.M., Moran, A., Abt, M.C., Beura, L.K., Lucas, P.J., Artis, D., Wherry, E.J., Hogquist, K., Vezys, V., Masopust, D., 2012. Antigen-independent differentiation and maintenance of effector-like resident memory T cells in tissues. J. Immunol. 188, 4866–4875.

Corgnac, S., Malenica, I., Mezquita, L., Auclin, E., Voilin, E., Kacher, J., Halse, H., Grynszpan, L., Signolle, N., Dayris, T., Leclerc, M., Droin, N., de Montpreville, V., Mercier, O., Validire, P., Scoazec, J.Y., Massard, C., Chouaib, S., Planchard, D., Adam, J., Besse, B., Mami-Chouaib, F., 2020. CD103(+)CD8(+) TRM cells accumulate in tumors of anti-PD-1-responder lung cancer patients and are tumor-reactive lymphocytes enriched with Tc17. Cell Rep. Med. 1, 100127.

Cuburu, N., Graham, B.S., Buck, C.B., Kines, R.C., Pang, Y.Y., Day, P.M., Lowy, D.R., Schiller, J.T., 2012. Intravaginal immunization with HPV vectors induces tissue-resident CD8+ T cell responses. J. Clin. Invest. 122, 4606–4620.

Djenidi, F., Adam, J., Goubar, A., Durgeau, A., Meurice, G., de Montpreville, V., Validire, P., Besse, B., Mami-Chouaib, F., 2015. CD8+CD103+ tumor-infiltrating lymphocytes are tumor-specific tissue-resident memory T cells and a prognostic factor for survival in lung cancer patients. J. Immunol. 194, 3475–3486.

Dolan, B.P., Li, L., Takeda, K., Bennink, J.R., Yewdell, J.W., 2010. Defective ribosomal products are the major source of antigenic peptides endogenously generated from influenza A virus neuraminidase. J. Immunol. 184, 1419–1424.

Edwards, J., Wilmott, J.S., Madore, J., Gide, T.N., Quek, C., Tasker, A., Ferguson, A., Chen, J., Hewavisenti, R., Hersey, P., Gebhardt, T., Weninger, W., Britton, W.J., Saw, R.P.M., Thompson, J.F., Menzies, A.M., Long, G.V., Scolyer, R.A., Palendira, U., 2018. CD103(+) tumor-resident CD8(+) T cells are associated with improved survival in immunotherapy-naive melanoma patients and expand significantly during anti-PD-1 treatment. Clin. Cancer Res. 24, 3036–3045.

Fernandez-Ruiz, D., Ng, W.Y., Holz, L.E., Ma, J.Z., Zaid, A., Wong, Y.C., Lau, L.S., Mollard, V., Cozijnsen, A., Collins, N., Li, J., Davey, G.M., Kato, Y., Devi, S., Skandari, R., Pauley, M., Manton, J.H., Godfrey, D.I., Braun, A., Tay, S.S., Tan, P.S., Bowen, D.G., Koch-Nolte, F., Rissiek, B., Carbone, F.R., Crabb, B.S., Lahoud, M., Cockburn, I.A., Mueller, S.N., Bertolino, P., McFadden, G.I., Caminschi, I., Heath, W. R., 2016. Liver-resident memory CD8(+) T cells form a front-line defense against malaria liver-stage infection. Immunity 45, 889–902.

Gebhardt, T., Wakim, L.M., Eidsmo, L., Reading, P.C., Heath, W.R., Carbone, F.R., 2009. Memory T cells in nonlymphoid tissue that provide enhanced local immunity during infection with herpes simplex virus. Nat. Immunol. 10, 524–530.

Gotch, F.M., McMichael, A.J., Smith, G., Moss, B., 1987. Identification of viral molecules recognized by Influenza-specific human cytotoxic T lymphocytes. J. Experimen. Med. 165, 408–416.

Hamdy, S., Haddadi, A., Hung, R.W., Lavasanifar, A., 2011. Targeting dendritic cells with nano-particulate PLGA cancer vaccine formulations. Adv. Drug. Deliv. Rev. 63, 943–955.

Hayward, S.L., Scharer, C.D., Cartwright, E.K., Takamura, S., Li, Z.T., Boss, J.M., Kohlmeier, J.E., 2020. Environmental cues regulate epigenetic reprogramming of airway-resident memory CD8(+) T cells. Nat. Immunol. 21, 309–320.

Herrmann, V.L., Hartmayer, C., Planz, O., Groettrup, M., 2015. Cytotoxic T cell vaccination with PLGA microspheres interferes with influenza A virus replication in the lung and suppresses the infectious disease. J. Control Release 216, 121–131.

Iijima, N., Iwasaki, A., 2015. Tissue instruction for migration and retention of TRM cells. Trends Immunol. 36, 556–564.

Jiang, X., Clark, R.A., Liu, L., Wagers, A.J., Fuhlbrigge, R.C., Kupper, T.S., 2012. Skin infection generates non-migratory memory CD8+ T(RM) cells providing global skin immunity. Nature 483, 227–231.

Johansen, P., Men, Y., Merkle, H.P., Gander, B., 2000. Revisiting PLA/PLGA microspheres: an analysis of their potential in parenteral vaccination. Eur. J. Pharm. Biopharm. 50, 129–146.

Kingstad-Bakke, B., Toy, R., Lee, W., Pradhan, P., Vogel, G., Marinaik, C.B., Larsen, A., Gates, D., Luu, T., Pandey, B., Kawaoka, Y., Roy, K., Suresh, M., 2021. Polymeric Pathogen-Like Particles-Based Combination Adjuvants Elicit Potent Mucosal T Cell Immunity to Influenza A Virus. Front. Immunol. 11.

Koerner, J., Horvath, D., Groettrup, M., 2019. Harnessing dendritic cells for poly (D,L-lactide-co-glycolide) microspheres (PLGA MS)-mediated anti-tumor therapy. Front. Immunol. 10, 707.

Koerner, J., Horvath, D., Herrmann, V.L., MacKerracher, A., Gander, B., Yagita, H., Rohayem, J., Groettrup, M., 2021. PLGA-particle vaccine carrying TLR3/RIG-I ligand Riboxxim synergizes with immune checkpoint blockade for effective anti-cancer immunotherapy. Nat. Commun. 12, 2935.

Koh, J., Kim, S., Kim, M.-Y., Go, H., Jeon, Y.K., Chung, D.H., 2017. Prognostic implications of intratumoral CD103+ tumor-infiltrating lymphocytes in pulmonary squamous cell carcinoma. Oncotarget 8, 13762–13769.

Komdeur, F.L., Prins, T.M., van de Wall, S., Plat, A., Wisman, G.B.A., Hollema, H., Daemen, T., Church, D.N., de Bruyn, M., Nijman, H.W., 2017. CD103+ tumor-infiltrating lymphocytes are tumor-reactive intraepithelial CD8+ T cells associated with prognostic benefit and therapy response in cervical cancer. Oncoimmunology 6, e1338230.

Krammer, F., Smith, G.J.D., Fouchier, R.A.M., Peiris, M., Kedzierska, K., Doherty, P.C., Palese, P., Shaw, M.L., Treanor, J., Webster, R.G., Garcia-Sastre, A., 2018. Influenza. Nat Rev Dis Primers 4, 3.

Mackay, L.K., Braun, A., Macleod, B.L., Collins, N., Tebartz, C., Bedoui, S., Carbone, F.R., Gebhardt, T., 2015. Cutting edge: CD69 interference with sphingosine-1-phosphate receptor function regulates peripheral T cell retention. J. Immunol. 194, 2059–2063.
Mackay, L.K., Stock, A.T., Ma, J.Z., Jones, C.M., Kent, S.J., Mueller, S.N., Heath, W.R., Carbone, F.R., Gebhardt, T., 2012. Long-lived epithelial immunity by tissue-resident memory T (TRM) cells in the absence of persisting local antigen presentation. Proc. Natl. Acad. Sci. U. S. A. 109, 7037–7042.
Marceaux, C., Weeden, C.E., Gordon, C.L., Marie-Liesse Asselin-Labat, M.-.L., 2021. Holding our breath: the promise of tissue-resident memory T cells in lung cancer. Transl. Lung Cancer Res. 10, 819–2829.
Masopust, D., Choo, D., Vezys, V., Wherry, E.J., Duraiswamy, J., Akondy, R., Wang, J., Casey, K.A., Barber, D.L., Kawamura, K.S., Fraser, K.A., Webby, R.J., Brinkmann, V., Butcher, E.C., Newell, K.A., Ahmed, R., 2010. Dynamic T cell migration program provides resident memory within intestinal epithelium. J. Exp. Med. 207, 553–564.
Matloubian, M., Lo, C.G., Cinamon, G., Lesneski, M.J., Xu, Y., Brinkmann, V., Allende, M. L., Proia, R.L., Cyster, J.G., 2004. Lymphocyte egress from thymus and peripheral lymphoid organs is dependent on S1P receptor 1. Nature 427, 355–360.
Matrosovich, M., Matrosovich, T., Garten, W., Klenk, H.D., 2006. New low-viscosity overlay medium for viral plaque assays. Virol. J. 3, 63.
McMaster, S.R., Wein, A.N., Dunbar, P.R., Hayward, S.L., Cartwright, E.K., Denning, T.L., Kohlmeier, J.E., 2018. Pulmonary antigen encounter regulates the establishment of tissue-resident CD8 memory T cells in the lung airways and parenchyma. Mucosal Immunol. 11, 1071–1078.
McMaster, S.R., Wilson, J.J., Wang, H., Kohlmeier, J.E., 2015. Airway-resident memory CD8 T cells provide antigen-specific protection against respiratory virus challenge through rapid IFN-gamma production. J. Immunol. 195, 203–209.
McMichael, A.J., Gotch, F.M., Noble, G.R., Beare, P.A.S., 1983. Cytotoxic T-cell immunity to influenza. N. Engl. J. Med. 309, 13–17.
Morris, M.A., Gibb, D.R., Picard, F., Brinkmann, V., Straume, M., Ley, K., 2005. Transient T cell accumulation in lymph nodes and sustained lymphopenia in mice treated with FTY720. Eur. J. Immunol. 35, 3570–3580.
Mueller, M., Reichardt, W., Koerner, J., Groettrup, M., 2012. Coencapsulation of tumor lysate and CpG-ODN in PLGA-microspheres enables successful immunotherapy of prostate carcinoma in TRAMP mice. J. Control Release 162, 159–166.
Mueller, M., Schlosser, E., Gander, B., Groettrup, M., 2011. Tumor eradication by immunotherapy with biodegradable PLGA microspheres–an alternative to incomplete Freund's adjuvant. Int. J. Cancer 129, 407–416.
Mueller, S.N., Mackay, L.K., 2016. Tissue-resident memory T cells: local specialists in immune defence. Nat. Rev. Immunol. 16, 79–89.
Muruganandah, V., Sathkumara, H.D., Navarro, S., Kupz, A., 2018. A systematic review: the role of resident memory T cells in infectious diseases and their relevance for vaccine development. Front. Immunol. 9.
Nizard, M., Roussel, H., Diniz, M.O., Karaki, S., Tran, T., Voron, T., Dransart, E., Sandoval, F., Riquet, M., Rance, B., Marcheteau, E., Fabre, E., Mandavit, M., Terme, M., Blanc, C., Escudie, J.B., Gibault, L., Barthes, F.L.P., Granier, C., Ferreira, L.C.S., Badoual, C., Johannes, L., Tartour, E., 2017. Induction of resident memory T cells enhances the efficacy of cancer vaccine. Nat. Commun. 8, 15221.
Okła, K., Farber, D.L., Zou, W., 2021. Tissue-resident memory T cells in tumor immunity and immunotherapy. J. Exp. Med. 218.
Park, C.O., Kupper, T.S., 2015. The emerging role of resident memory T cells in protective immunity and inflammatory disease. Nat. Med. 21, 688–697.
Pauls, K., Schon, M., Kubitza, R.C., Homey, B., Wiesenborn, A., Lehmann, P., Ruzicka, T., Parker, C.M., Schon, M.P., 2001. Role of integrin alphaE(CD103)beta7 for tissue-specific epidermal localization of CD8+ T lymphocytes. J. Invest. Dermatol. 117, 569–575.
Ribas, A., Wolchok, J.D., 2018. Cancer immunotherapy using checkpoint blockade. Science 359, 1350–1355.
Sallusto, F., Geginat, J., Lanzavecchia, A., 2004. Central memory and effector memory T cell subsets: function, generation, and maintenance. Annu. Rev. Immunol. 22, 745–763.
Sandoval, F., Terme, M., Nizard, M., Badoual, C., Bureau, M.-F., Freyburger, L., Clement, O., Marcheteau, E., Gey, A., Fraisse, G., Bouguin, C., Merillon, N., Dransart, E., Tran, T., Quintin-Colonna, F., Autret, G., Thiebaud, M., Suleman, M., Riffault, S., Wu, T.-.C., Launay, O., Danel, C., Taieb, J., Richardson, J., Zitvogel, L., Fridman, W.H., Johannes, L., Tartour, E., 2013. Mucosal imprinting of vaccine-induced CD8+ T cells is crucial to inhibit the growth of mucosal tumors. Sci. Transl. Med. 5.
Schenkel, J.M., Fraser, K.A., Masopust, D., 2014. Cutting edge: resident memory CD8 T cells occupy frontline niches in secondary lymphoid organs. J. Immunol. 192, 2961–2964.
Schenkel, J.M., Fraser, K.A., Vezys, V., Masopust, D., 2013. Sensing and alarm function of resident memory CD8(+) T cells. Nat. Immunol. 14, 509–513.
Schliehe, C., Redaelli, C., Engelhardt, S., Fehlings, M., Mueller, M., van Rooijen, N., Thiry, M., Hildner, K., Weller, H., Groettrup, M., 2011. CD8- dendritic cells and macrophages cross-present poly(D,L-lactate-co-glycolate) acid microsphere-encapsulated antigen *in vivo*. J. Immunol. 187, 2112–2121.
Schlosser, E., Mueller, M., Fischer, S., Basta, S., Busch, D.H., Gander, B., Groettrup, M., 2008. TLR ligands and antigen need to be coencapsulated into the same biodegradable microsphere for the generation of potent cytotoxic T lymphocyte responses. Vaccine 26, 1626–1637.
Shin, H., Iwasaki, A., 2012. A vaccine strategy that protects against genital herpes by establishing local memory T cells. Nature 491.
Shiow, L.R., Rosen, D.B., Brdickova, N., Xu, Y., An, J., Lanier, L.L., Cyster, J.G., Matloubian, M., 2006. CD69 acts downstream of interferon-alpha/beta to inhibit S1P1 and lymphocyte egress from lymphoid organs. Nature 440, 540–544.
Slütter, B., Van Braeckel-Budimir, N., Abboud, G., Varga, S.M., Salek-Ardakani, S., Harty, J.T., 2017. Dynamics of influenza-induced lung-resident memory T cells underlie waning heterosubtypic immunity. Sci. Immunol. 2, eaag2031.
Takamura, S., 2017. Persistence in Temporary Lung Niches: a Survival Strategy of Lung-Resident Memory CD8+ T Cells. Viral Immunol. 30, 438–450.
Takamura, S., 2018. Niches for the Long-Term Maintenance of Tissue-Resident Memory T Cells. Front. Immunol. 9.
Takamura, S., Yagi, H., Hakata, Y., Motozono, C., McMaster, S.R., Masumoto, T., Fujisawa, M., Chikaishi, T., Komeda, J., Itoh, J., Umemura, M., Kyusai, A., Tomura, M., Nakayama, T., Woodland, D.L., Kohlmeier, J.E., Miyazawa, M., 2016. Specific niches for lung-resident memory CD8+ T cells at the site of tissue regeneration enable CD69-independent maintenance. J. Exp. Med. 213, 3057–3073.
Uddback, I.E.M., Pedersen, L.M.I., Pedersen, S.R., Steffensen, M.A., Holst, P.J., Thomsen, A.R., Christensen, J.P., 2016. Combined local and systemic immunization is essential for durable T-cell mediated heterosubtypic immunity against influenza A virus. Scient. Rep. 6, 20137.
Van Braeckel-Budimir, N., Varga, S.M., Badovinac, V.P., Harty, J.T., 2018. Repeated antigen exposure extends the durability of influenza-specific lung-resident memory CD8+ T cells and heterosubtypic immunity. Cell Rep. 24, 3374–3382.
Vasir, J.K.L., 2007. Biodegradable nanoparticles for cytosolic delivery of therapeutics. Adv. Drug. Deliv. Rev. 59, 718–728.
Waeckerle-Men, Y., Groettrup, M., 2005. PLGA microspheres for improved antigen delivery to dendritic cells as cellular vaccines. Adv. Drug. Deliv. Rev. 57, 475–482.
Wakim, L.M., Waithman, J., van Rooijen, N., Heath, W.R., Carbone, F.R., 2008. Dendritic cell–induced memory t cell activation in nonlymphoid tissues. Science 319, 198–202.
Wakim, L.M., Woodward-Davis, A., Bevan, M.J., 2010. Memory T cells persisting within the brain after local infection show functional adaptations to their tissue of residence. Proc. Natl. Acad. Sci. U. S. A. 107, 17872–17879.
Wong, S.S., Webby, R.J., 2013. Traditional and new influenza vaccines. Clin. Microbiol. Rev. 26, 476–492.
Wu, T., Hu, Y., Lee, Y.-.T., Bouchard, K.R., Benechet, A., Khanna, K., Cauley, L.S., 2014. Lung-resident memory CD8 T cells (TRM) are indispensable for optimal crossprotection against pulmonary virus infection. J. Leukoc. Biol. 95, 215–224.
Zaid, A., Mackay, L.K., Rahimpour, A., Braun, A., Veldhoen, M., Carbone, F.R., Manton, J.H., Heath, W.R., Mueller, S.N., 2014. Persistence of skin-resident memory T cells within an epidermal niche. Proc. Natl. Acad. Sci. U. S. A. 111, 5307–5312.
Zens, K.D., Chen, J.K., Farber, D.L., 2016. Vaccine-generated lung tissue-resident memory T cells provide heterosubtypic protection to influenza infection. JCI Insight 1.